

**SU-8 PIEZORESISTIVE MICROCANTILEVER FOR CHEMICAL SENSING
APPLICATION**

by

LEE KOK SIONG

**Thesis submitted in fulfillment of the requirements
for the degree of
Master of Science**

MAY 2011

ACKNOWLEDGEMENTS

I would like to express my deepest and sincere gratitude to my supervisor, Associate Professor Dr. Ishak Bin Haji Abdul Azid for his tremendous guidance and support throughout my postgraduate candidature period. His words of wisdom and positive thinking have been a great value for me. Also my special thanks to my co-supervisors, Professor Kamarulazizi Bin Ibrahim and Dr. Mutharasu Devarajan from Nano-Optoelectronic Research and Technology (N.O.R) Lab for their guidance and useful ideas in handling and exploring the fabrication works.

I wish to express my warm and sincere thanks to my colleagues, Mr. Wong Wah Seng and Ms. Wong Wai Chi for their grateful discussions, useful suggestions, and assistance on my research work. Apart from them, I would like to forward special thanks to N.O.R Lab technical staffs Madam Bee Cho, Mr. Mokhtar, Mr. Jamil, and Mr. Hazhar for their countless efforts in helping me to complete my research. Thanks are also to all students and staffs of Universiti Sains Malaysia (USM), those who helped me either directly or indirectly for this project.

Not to forget, my ever-loving parents and family who always are on my side, sharing my ups and downs. They have given me inspiration to work hard and motivated me during this research work. Last but not the least, I gratefully appreciate the Institute of Postgraduate Studies (IPS) for awarding me the USM Fellowship which relieved me of financial insecurity.

Lee Kok Siong

May 2011

TABLE OF CONTENTS

Acknowledgements	ii
Table Of Contents	iii
List Of Tables	vii
List Of Figures	viii
List Of Symbols	xiii
List Of Abbreviations	xiv
Abstrak	xv
Abstract	xvi
CHAPTER 1 - INTRODUCTION	
1.0 Overview	1
1.1 Background of Cantilever Sensors	1
1.2 Biochemical cantilever based sensors	3
1.3 SU-8 as structural material	4
1.4 Readout method	5
1.5 Problem statement	6
1.7 Research Objectives	8
1.8 Thesis outline	8
CHAPTER 2 - LITERATURE REVIEW	
2.0 Overview	9
2.1 Sensor classification	9
2.2 Piezoresistive microcantilever for chemical sensing	11
2.2.1 Piezoresistive readout concept	12
2.2.2 Wheatstone bridge configuration	13
2.2.3 Piezoresistive material	14
2.2.4 Existing piezoresistive microcantilever for surface stress measurement	17
2.3 Design consideration	18
2.3.1 Cantilever shape	19
2.3.2 Sensitivity enhancement	21
2.4 Finite element analysis	25
2.5 Fabrication of SU-8 microcantilevers	27
2.5.1 Typical SU-8 photolithography process	27
2.5.2 Typical SU-8 microcantilever process	27

2.5.3	Releasing SU-8 structures	30
2.6	Remarks on the literature survey	31
2.7	Summary	33

CHAPTER 3 - THEORY

3.0	Overview	34
3.1	Basic mechanic	34
3.2	Different strain cases	37
3.2.1	Free end force on cantilever beam	38
3.2.2	Free end force on cantilever plate	38
3.2.3	Biaxial in-plane stress on cantilever beam	39
3.2.4	Biaxial in-plane stress on cantilever plate	39
3.3	Deflection sensitivity for piezoresistive cantilever	39
3.4	Surface stress sensitivity for piezoresistive cantilever	40
3.5	Summary	42

CHAPTER 4 - DESIGN & FABRICATION OF SU-8 MICROCANTILEVER

4.0	Overview	43
4.1	Design consideration	43
4.2	Finite Element (FE) Analysis with ANSYS®	44
4.2.1	Finite element modeling in ANSYS®	45
4.2.2	System of units	47
4.2.3	Element type	48
4.2.4	Material properties	48
4.2.5	Meshing	49
4.2.6	Merge operation	51
4.2.7	Boundary conditions	51
4.2.8	Surface stress loading	52
4.3	Sensors design	53
4.3.1	1st Design: Single pair microcantilever	54
4.3.2	2nd Design: Array of microcantilever	56
4.3.3	Material selection	57
4.3.4	Mask layout	58
4.4	Fabrication process	61
4.4.1	Mask plotting	63
4.4.2	Substrate preparation	64

4.4.3	Photolithography	65
4.4.4	Al etching	72
4.4.5	Deposition of SU-8/Ag composite	74
4.4.6	Pt lift-off	76
4.4.7	SU-8 releasing process	78
4.4.8	Adhesive bonding to thick support base	79
4.5	Characterization/experimental setup	80
4.5.1	Material properties of fabricated SU-8	80
4.5.2	Surface investigations	81
4.5.3	Assessment of release method	82
4.5.4	Characterization of piezoresistors	84
4.5.5	Electromechanical characterization of SU-8 microcantilever	85
4.5.6	Hydrogen gas detection	86
4.6	Summary	87
CHAPTER 5 - RESULTS AND DISCUSSIONS		
5.0	Overview	88
5.1	Finite Element Analysis with ANSYS®	88
5.1.1	Verification of simulation procedures	88
5.1.2	Thickness of insulation layers	90
5.1.3	Thickness of piezoresistor	92
5.1.4	Cantilever length	94
5.1.5	L/W ratio	95
5.1.6	Piezoresistor layout	96
5.1.7	Design guidelines	98
5.1.8	Remarks for FEA	98
5.2	Characterization of fabrication process	99
5.2.1	Substrate selection	99
5.2.2	Assessment of release methods	101
5.2.3	Material properties	106
5.2.4	AFM investigation	108
5.2.5	Failure analysis	111
5.3	Cantilever measurement	117
5.3.1	I-V test for SU-8/Ag piezoresistor	117
5.3.2	Deflection test	118
5.3.3	Cantilever performance	119

5.4	Application testing	125
5.5	Summary	127
CHAPTER 6 - CONCLUSIONS		
6.0	Conclusions	128
6.1	Recommendation for future works	129
BIBLIOGRAPHY		130
PUBLICATION LIST		138

LIST OF TABLES

		PAGE
Table 2.1	Existing piezoresistive microcantilever sensors for surface stress detection	17
Table 2.2	Summary of cantilever shape from literatures	20
Table 2.3	Summary of available approaches in enhance the sensitivity	24
Table 2.4	Literature summary of FEA using ANSYS® for piezoresistive microcantilever under surface stress loading	26
Table 2.5	Literatures that used flip-chip approach for device fabrication	29
Table 2.6	The drawbacks of existing dry release method	31
Table 4.1	Mechanical conversion factors for MKS to μ MKSV	47
Table 4.2	Material properties for SU-8 and Gold	49
Table 4.3	Nominal dimensions, element sizes and total element for FE model	50
Table 4.4	Cantilever thickness	55
Table 4.5	Explanation of the mask sets	58
Table 4.6	Chemical solution for photosensitive film cleaning	64
Table 4.7	Spin speeds and accelerations in the SU-8 processing with resulting thicknesses	66
Table 4.8	Spin speeds and accelerations for primer and PR1-1000A resist	68
Table 4.9	Soft baking times at different temperatures for different thicknesses of resists	69
Table 4.10	Energy dosage for exposure for different thicknesses of resists	70
Table 4.11	PEB times at different temperatures for different thicknesses of SU-8	71
Table 5.1	The thickness of insulation layers with corresponding thickness ratio	89
Table 5.2	Comparison between two release methods	106
Table 5.3	Tensile test result	107
Table 5.4	AFM results of five samples prepared	108
Table 5.5	Value of parameters used for solving equation 5.3-4	122

Table 5.6	Overview of cantilever performance	124
Table 5.7	Comparison of surface stress sensitivity	124

LIST OF FIGURES

		PAGE
Figure 1.1	Schematic illustration of the AFM detection system (Eriksen, 2002)	2
Figure 1.2	Cantilever is deflected due to the generated surface stress as the molecules bind on the immobilized layer (Nordström et al., 2008)	4
Figure 1.3	High aspect ratio structures achieved with SU8 (Microchem) (a) SU-8 gears (b) SU-8 pixel walls	5
Figure 1.4	Readout Method: (a) optical (Zheng et al., 2008); (b) piezoresistive (Thaysen et al., 2000); (c) capacitive (Napoli et al., 2004)	6
Figure 2.1	Schematic of chemical sensing process	10
Figure 2.2	Scheme of analyte binds selectively to the functionalized cantilever (Nordström, 2008)	11
Figure 2.3	Schematic of a Wheatstone bridge. The resistor placed inside the cantilever used for measuring is denoted R_{cant} . The supply voltage is denoted V_{in} and the output voltage V_{out}	13
Figure 2.4	Optical microscope image of the thermally symmetrical Wheatstone bridge configuration (Thaysen et al., 2000)	14
Figure 2.5	As the cantilever is strained, contact is broken between the conducting particles in the polymer and the resistance of the conductor is thereby increased (Nordström, 2008)	16
Figure 2.6	The cantilever exhibits a constant curvature in places where surface stress is applied and remains straight at non-surface stress area (Thaysen, 2001)	18
Figure 2.7	Types of microcantilever shape, (a) Rectangular (Loui et al., 2008), (b) Paddle type (Su et al., 1996), (c) V-shaped (Saya et al., 2005), (d) T-shaped (Plaza et al., 2006), (e) U-shaped (Villanueva et al., 2004)	21
Figure 2.8	The double-microcantilever design composed of the functionalized microcantilever, measuring microcantilever, and the connecting transmitter (Yang et al., 2006)	24
Figure 2.9	Typical SU-8 photolithography process	27

Figure 2.10	Typical fabrication process of the SU-8 cantilever (Thaysen et al., 2002)	28
Figure 2.11	Low step coverage proved to be a major problem when using flip-chip approach in fabricating SU-8 microcantilever	29
Figure 3.1	Free end force acting on a cantilever	35
Figure 3.2	Cross-sectional schematic of a cantilever experiencing a free end force	36
Figure 3.3	Cross-section of a composite cantilever with i 'th layers	37
Figure 3.4	Stress-strain planes for three dimensions cantilever	38
Figure 3.5	Schematic diagram of a three-layered piezoresistive microcantilever	41
Figure 4.1	Conceptual design of SU-8 piezoresistive microcantilever (a) Top view (b) Section view and isometric view in the thumbnail	45
Figure 4.2	Geometry of piezoresistor and direction of the current I flow through the resistor. The resistance of transverse part (hatched) is much lower than longitudinal resistance	46
Figure 4.3	Top view of the final FE model used in the analysis	47
Figure 4.4	FE model meshed by mapped meshing with hexahedral shaped	50
Figure 4.5	The same element size for touching regions will generate coincident nodes. The touching regions can then be combined by execute the NUMMRG command in ANSYS®	51
Figure 4.6	Boundary condition at one cantilever end to replace the function of substrate	52
Figure 4.7	Free end displacement induced by 0.5 N/m surface stress	53
Figure 4.8	Wiring of cantilever sensor and resistors configuration in the Wheatstone bridge	54
Figure 4.9	Cantilever structure (a) Cross section view (b) Top view of the cantilever	55
Figure 4.10	Design of microcantilever array, the resistors on the substrate is indicated by dashed oval	56
Figure 4.11	The dimension and surface area of the cantilever array	57
Figure 4.12	Mask set for first sensor design	59
Figure 4.13	Mask set for second sensor design	60

Figure 4.14	Process sequence	62
Figure 4.15	General photolithography process; (a) Deposition of resist (b) UV-exposure (c) resist developed	64
Figure 4.16	SU-8 2000 Spin Speed versus Thickness (MicroChem)	67
Figure 4.17	SU-8 structures after development process	72
Figure 4.18	PR1-1000A layer on top of Al layer	73
Figure 4.19	Al patterning on top of SU-8 layer	73
Figure 4.20	Electrical conductivity of SU-8/Ag for various silver volume fractions (Jinguet et al., 2004)	74
Figure 4.21	SU-8/Ag was patterned using backside UV exposure	75
Figure 4.22	The pattern of SU-8/Ag composite	76
Figure 4.23	Sputtering machine	77
Figure 4.24	Optical image of the cantilever coated with Platinum	77
Figure 4.25	Release process flow using the transparency substrate	78
Figure 4.26	Bonding process	79
Figure 4.27	Final SU-8 device; (a) Support layer used in bonding process (b) Device after the bonding process	80
Figure 4.28	Size of test specimen	81
Figure 4.29	Bubble buoyant force release method (a) Substrate coated with thin carbon film as sacrificial layer, (b) Spin-on and lithography of SU-8 photoresist, (c) Resist development, (d) Immersion of the specimen in boiled DI water, (e) Structure released by bubble buoyant force	83
Figure 4.30	I-V test setup: (a) test setup system, (b) Point probe setup (c) Point probe connected to I-V tester	84
Figure 4.31	Deflection test setup	85
Figure 4.32	Cantilever deflects when the sharp needle was moved downward	85
Figure 4.33	Schematic of the experimental test apparatus. Pairs of each piezoresistive cantilever design are exposed to the 5% H ₂ . The voltage output (V _o) was measured using multimeter	86
Figure 4.34	Hydrogen gas detection setup	87
Figure 5.1	Comparison between the ANSYS and analytical results	90

Figure 5.2	The effect of insulation layers thickness on piezoresistive strain for (a) fixed cantilever thickness (b) fixed top insulation layer thickness	91
Figure 5.3	The position of the piezoresistive layer with respect to the mid plane, due to the change of thickness ratio t_3/t_1	91
Figure 5.4	Piezoresistor strain vs. the thickness of resistors for cantilever with surface stress loading	93
Figure 5.5	(a) Strain distribution on top of cantilever (b) Piezoresistive strain vs. cantilever length for cantilever under surface stress loading	94
Figure 5.6	(a) The surface area of cantilevers is kept constant (b) Width dependence of piezoresistive strain for cantilevers under surface stress loading	95
Figure 5.7	Piezoresistor layout dependence of piezoresistive strain for different cantilever width (a) piezoresistor length (b) width of piezoresistive region	97
Figure 5.8	(a) The SU-8 patterned on the glass substrate were disordered after developed with PGMEA (b) SU-8 on the transparency substrate shows the desired pattern faithfully	100
Figure 5.9	Series of time-resolved photographs showing the SU-8 structure release dynamics using the bubble force release method. The cantilevers are 0.5 mm wide and 1.5 mm long (Releasing time: 10 s)	102
Figure 5.10	Released SU-8 membrane with thickness of 150 μm , area of 100 mm^2 and 225 m^2 (Releasing time: 30 s and 38 s)	103
Figure 5.11	Graph undercut vs. time curve	104
Figure 5.12	SEM images of single layer SU-8 cantilever structure released by buoyant force release method (a) before release, and (b) after release	104
Figure 5.13	SEM images of single layer SU-8 cantilever structure released by transparency dry release method (a) before release, and (b) after release	105
Figure 5.14	(a) The specimens prepared for tensile test (b) Tested specimen break at grip area	107
Figure 5.15	Graph load vs. extension	107
Figure 5.16	3D images generated by AFM testing	109
Figure 5.17	Over-etched Aluminum during wet etching process	112
Figure 5.18	Under-etched Aluminum during wet etching process	112

Figure 5.19	Aluminum layer has wrinkles after immersed into Acetone solution	113
Figure 5.20	Mishandling the fabricated piezoresistive microcantilever	114
Figure 5.21	Misalignment of the SU-8 layers	114
Figure 5.22	The pattern of SU-8/Ag composite after developed (a) without ultrasonication (b) with ultrasonication	116
Figure 5.23	Current-voltage (I-V) plots and the resistances for fabricated piezoresistors	117
Figure 5.24	Endpoint deflection of the SU-8 cantilever fabricated. (a) The offset occurred due to unequal resistance (b) The data has been offset-subtracted and multiplied by -1	118
Figure 5.25	The relative change in resistance as a function of the cantilever deflection. The two lines represent the two steps in the deflection test, deflection and release	119
Figure 5.26	The neutral axis of unify cantilever located at the middle of cantilever	120
Figure 5.27	Two types of stresses acting on measurement cantilever when exposed to a surface stress on the front side. The front side exhibits higher strain than backside	123
Figure 5.28	Photomicrograph of three cantilever pairs with different dimension designed	125
Figure 5.29	Voltage versus time of the cantilever array to 5% H ₂ exposure. The data has been offset-subtracted and multiply by -1	126

LIST OF SYMBOLS

SYMBOL	DESCRIPTION	UNIT
R	Resistance	Ω
σ_s	Surface stress	N/m
$\Delta R/R$	Relative change in resistance	-
S	Surface stress sensitivity	$[\text{N/m}]^{-1}$
G_f	Gauge factor	-
ε	Strain	-
V	Voltage	Volt
ρ	Resistivity	Ωm
ν	Poisson's ratio	-
π	Piezoresistive coefficient	-
σ	Stress	Pa
E	Young's modulus	Pa
k	Spring constant	N/m
L	Length	m
t	Thickness	m
u	Deflection	m
F	Force	N
M	Bending moment	Nm
I	Area moment of inertia	m^4
z_N	Neutral axis	m
L/W	Length to width ratio	-
z_i	Center position of the i 'th layer	m
A	Area	m^2
z	Distance to the neutral axis	m
W	Width	m
d	Distance between the resistor and the neutral axis	m
λ	Length of resistor	m
Y	Biaxial modulus for a beam or Plate modulus for a plate	Pa
n	Number of turn	-
D	Distance between resistor legs	m
I	Current	amp
$(\Delta R/R). u^{-1}$	Deflection sensitivity	m^{-1}

LIST OF ABBREVIATIONS

AFM	Atomic force microscope
3-D	Three-dimensional
MEMS	Micro electro-mechanical systems
IBM	International business machines
UV	Ultraviolet
Si	Silicon
FEA	Finite element analysis
Ag	Silver
SiO ₂	Silicon dioxide
SCR	Stress concentration region
CAD	Computer aided design
PEB	Post exposure bake
Cr	Chromium
Al	Aluminum
PCB	Print circuit board
Pt	Platinum
CTE	Coefficient of thermal expansion
APM	Ammonia peroxide mixture
NH ₄ OH	Ammonium hydroxide
H ₂ O ₂	Hydrogen peroxide
DI	Deionize
N ₂	Nitrogen gas
SEM	Scanning electron microscope
HMDS	Hexamethyldisilazane
PGMEA	Propylene glycol methyl ether acetate
IPA	Isopropyl alcohol
HF	Hydrogen fluoride
H ₂	Hydrogen gas
Au	Gold

MIKRORASUK SU-8 PIEZORESISTIF UNTUK APLIKASI SEBAGAI PENDERIA KIMIA

ABSTRAK

Dalam penyelidikan ini, satu jenis bahan polimer yang boleh dibentuk oleh ultraungu, SU-8 dengan modulus Young yang sangat rendah berbanding dengan silikon digunakan sebagai bahan struktur mikrorasuk untuk meningkatkan terikan piezoresistif. Selain itu, Analisis Elemen Terhingga (FEA) secara menyeluruh telah dilakukan untuk mikrorasuk SU-8 piezoresistif di bawah tegangan permukaan supaya membantu dalam peningkatkan terikan piezoresistif semasa mereka penderia rasuk. Keputusan analisis menyimpulkan bahawa rasuk SU-8 piezoresistif untuk penderiaan kimia harus mempunyai nisbah panjang ke lebar (L/W) yang lebih rendah untuk mendapat terikan piezoresistif yang lebih tinggi. Terdapat dua jenis rasuk direka yang telah difabrikasi dan diuji dalam kajian ini: pasangan rasuk dan barisan rasuk. Untuk dua jenis rekaan ini, SU-8/Perak (Ag) komposit telah tertanam ke dalam rasuk sebagai piezoresistor. Selain itu, penderia mikrorasuk adalah difabrikasi dengan menggunakan kaedah "ikatan pelekat", dan bukan "flip-chip" yang konvensional. Keputusan daripada Scanning Electron Microscope (SEM), Atomic Force Microscopy (AFM), dan ujian tegangan membuktikan bahawa kerja fabrikasi sangat baik dijalankan. Selanjutnya, daripada ujian arus-voltan (I-V), piezoresistor yang difabrikasi menunjukkan ciri perintang yang linear dengan konduktiviti yang baik. Selepas ujian lendutan, pekali terikan yang dikira adalah setinggi 26.3 dan mempunyai kepekaan tegangan permukaan $1.28 \times 10^{-3} \text{ [N/m]}^{-1}$ untuk rasuk yang berdimensi $800 \mu\text{m} \times 800 \mu\text{m}$. Barisan rasuk mengandungi tiga pasangan rasuk dengan L/W yang berlainan telah digunakan untuk mengesan gas H_2 . Keputusan menunjukkan bahawa pasangan rasuk dengan L/W terendah (0.79) mengeluarkan output voltan yang tertinggi, di mana menyamai dengan keputusan FEA.

SU-8 PIEZORESISTIVE MICROCANTILEVER FOR CHEMICAL SENSING APPLICATION

ABSTRACT

In this research, the ultraviolet (UV) patternable polymer material, SU-8 with very low Young's modulus compared to conventional silicon based material, is utilized as structural material for microcantilever to enhance the piezoresistive strain. In addition to that, a thorough Finite Element Analysis (FEA) has been carried out for SU-8 piezoresistive microcantilever under the surface stress loading to help in improving the piezoresistive strain when designing the cantilever sensor. The analysis result concluded that the SU-8 cantilevers for chemical sensing should have lower length to width (L/W) ratio for higher piezoresistive strain. There are two cantilever designs that have been fabricated and characterized in this research: single pair cantilever and array of cantilever. For these designs, the SU-8/Silver (Ag) composite has been embedded into the cantilever as piezoresistor. Besides, the cantilever sensors were fabricated using the adhesive bonding method, instead of the conventional flip-chip approach. The results from Scanning Electron Microscope (SEM), Atomic Force Microscopy (AFM), and tensile tests proved that the fabrication works were very well carried out. Furthermore, from current-voltage (I-V) test, the fabricated piezoresistors exhibit the linear resistance characteristic with good conductivity. After deflection test, the calculated gauge factor is as high as 26.3, which induced the surface stress sensitivity of $1.28 \times 10^{-3} \text{ [N/m]}^{-1}$ for nominal $800 \text{ }\mu\text{m} \times 800 \text{ }\mu\text{m}$ microcantilever. Microcantilever array with three different L/W cantilever pairs have been used for H_2 gas detection to examine the functionality of fabricated cantilever in chemical sensing application. From the result, the cantilever pair with the lowest L/W (0.79) exhibits the highest voltage output, which agrees with the FEA result.

CHAPTER 1

INTRODUCTION

1.0 Overview

In this section an introduction to the microcantilever sensor, along with basic operation concepts, problem definition, the objectives and the outline of the thesis, will be presented. The main contents in this chapter are:

- Background of cantilever sensors
- Biochemical cantilever based sensors
- SU-8 as structural material
- Readout method
- Problem statement
- Research objectives
- Thesis outline

1.1 Background of Cantilever Sensors

After the invention of the atomic force microscope (AFM) by Binnig et al. in 1986, there has been an increase in using microcantilevers to measure forces. Basically, AFM consists of a tiny cantilever beam (typical size: 200 μm x 100 μm) that is brought in contact with a sample. **Figure 1.1** shows a schematic of a generic AFM probe with a tip at its end. When the sample is moved very close to the cantilever tip during the operation, the Van der Waals forces between tip and sample will bend the cantilever. This deflection can be detected by an optical readout system consisting of a laser beam, which focuses on the cantilever and reflects onto a different spot on a deflection sensor (Eriksen, 2002). While scanning the sample in the x and y direction, a feedback system ensures a constant distance between sample and tip is obtained by moving the sample in z direction. By mapping the sample position, the topography of three-dimensional (3-D) modeling image of the sample can be acquired.

Soon after the invention of AFM, micromachining techniques (Madou, 1997) were used to make cantilevers in materials widely used in the microelectronics industry like silicon, silicon oxide and silicon nitride (Albrecht et al., 1987; Binnig et al., 1987), making it possible to fabricate cantilevers in micron size. The microcantilever sensors developed for AFM have proven their ability in measuring physical quantities other than the force interactions from the AFM measurements. For instances, the detection of heat fluxes causing the cantilever to bend due to the bimetallic effect as reported by Gimzewski et al. (1994), the measurement of mass changes through the change in resonant frequency of a cantilever caused by the adsorbed mass as reported by Thundat et al. (1994), and protein detection via measuring the cantilever deflection induced by antigen–antibody molecular recognition as reported by Arntz et al. (2003).

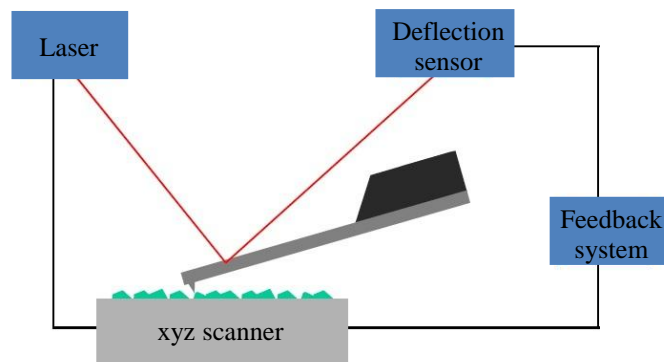


Figure 1.1 Schematic illustration of the AFM detection system (Eriksen, 2002)

When using the cantilever as a biochemical sensor the mechanical system turns out to be simpler. The surface to investigate is now the surface of the cantilever, thus the feedback and scanning system is not required. Brugger et al. (1999) and Thundat et al. (1995) have claimed that cantilever based sensors are the simplest device among Micro Electro-Mechanical Systems (MEMS) devices that offer great prospects for the development of novel physical and biochemical sensors.

1.2 Biochemical Cantilever Based Sensors

The large surface to volume ratio enables the surface related force such as the surface tension, capillary force, or surface energy to induce mechanical responses (Yin, 2005). Surface stresses generated due to adsorption of molecules on cantilevers surface were reported by Raiteri et al. and Chen et al. in 1995; Butt in 1996, and this exhibits the potential use of microcantilevers in biochemical sensing application. For such sensing purpose, one side of the cantilever is typically functionalized by coating an immobilized layer on cantilever top. In the presence of chemical species, this layer will undergoes volumetric expansion or contraction and results in microcantilever deformation. The static deflection from biochemical reaction can thus be measured with a proper readout method. Major advantages of the direct detection on the cantilever are (Rasmussen, 2003):

- In situ measurements as surface stress change.
- Enable of label-free detection so that the molecules to be detected do not need pre-treatments.

The microcantilever can be operated either in dynamic mode or static mode. In the dynamic mode the resonance frequency of the cantilever is monitored, in which the resonance frequency decreases as masses adsorb onto the structure. Chen et al. (1995) made a measurement on resonating cantilevers and proved that the change in resonant frequency was induced by added mass and the change in spring constant during adsorption. Besides, most biochemical measurements are performed in liquid. As a result, dynamic mode operation is difficult due to viscous damping that lower the frequency resolution (Nordström et al., 2008). Therefore, this research is focused only on static mode operation to ensure the cantilever sensor works well in both liquid and gaseous environment.

In the static mode, the cantilever is deformed due to the surface stress generated when molecules selectively adsorb onto one cantilever surface. **Figure 1.2** shows this principle schematically. The cantilever bending due to the adsorption measurements have been reported by many biochemical systems. For instances, the detection of the self-

assembly of alkanethiols by Berger et al.(1997) and the antibody binding detection by Raiteri et al. (1999) and Kim et al. (2003).

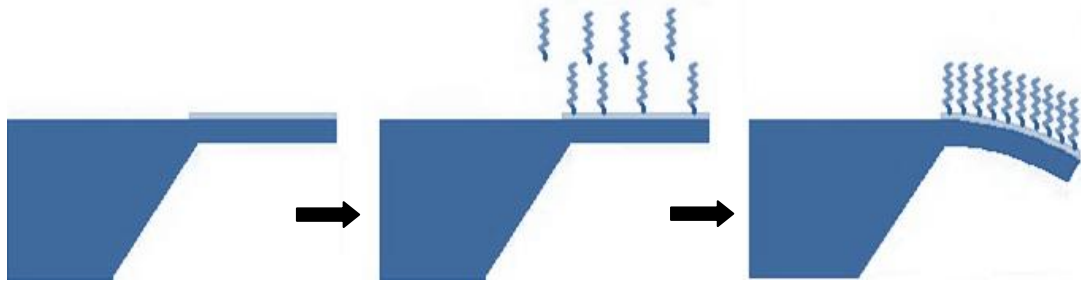


Figure 1.2 Cantilever is deflected due to the generated surface stress as the molecules bind on the immobilized layer (Nordström et al., 2008)

1.3 SU-8 As Structural Material

In MEMS field, the devices are conventionally fabricated in silicon (Si) related materials but recently polymer has arisen as a promising alternative material, especially SU-8. SU-8 is an epoxy-based negative photoresist developed by International Business Machines (IBM), which crosslinks upon ultraviolet (UV) exposure. Due to the useful material properties of SU-8 such as photosensitive, low Young's modulus, chemically resistant and biocompatible, it has become a popular and low-cost alternative to silicon for the fabrication of passive components. It offers a flexible platform for component design and has wide applications, which makes it very interesting as it is also compatible with standard Si processing equipment.

The good chemical compatibility and biocompatibility makes SU-8 an excellent material selection for microdevices. The fabrication of free-standing structures such as polymeric microcantilevers also present some advantages over silicon. Example is the reduction of actuation voltage required for a SU-8 electrostatic actuator due to the lower Young's modulus (Abgrall et al., 2007). SU-8 has also gained an enormous interest due to its ability to define layers from thicknesses $<1\mu\text{m}$ to 2mm with high aspect ratio (>20). Layers of a few hundred of microns can be simply spin-coated and patterned via conventional UV exposure systems. **Figure 1.3** shows high aspect ratio structures achieved with SU-8. It is therefore well suited for thick-film applications and it has been used as structural material in

micro- and nanotechnology. The use of a photoresist as a structural material also represents new opportunities in system integration. In this research, work on fabricating cantilevers for chemical detection in SU-8 is presented.

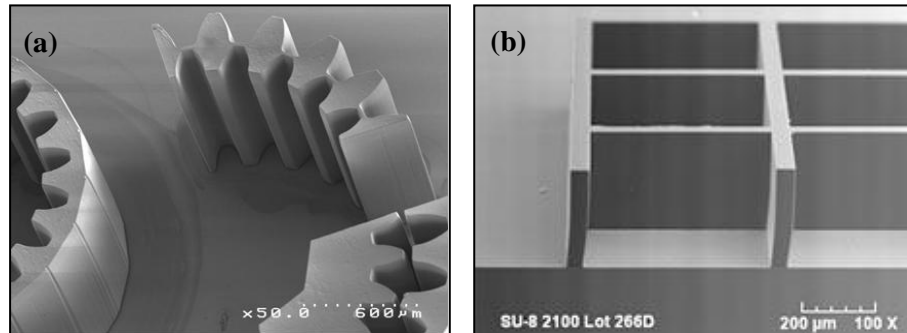


Figure 1.3 High aspect ratio structures achieved with SU8 (Microchem) (a) SU-8 gears (b) SU-8 pixel walls

1.4 Readout Method

The displacement or bending of microcantilevers for biochemical sensing application is related to the change in surface stress as mentioned earlier in **Section 1.2**. By monitoring the cantilever deflection, the change in surface stress can be detected. Yue et al. (2004) and Raiteri et al. (2001) mentioned that the cantilever deflection is commonly measured using optical, capacitive, and piezoresistive methods as illustrated in **Figures 1.4**.

Microcantilever deflection is most commonly measured by reflecting a laser from the free end of the cantilever. However, the need for a laser and external optics is obviated in the cases of capacitive and piezoresistive readout method. The capacitive readout method is based on the change in capacitance when cantilever is bending. It is widely used in microaccelerometers and microsensors for harsh environment (Firdaus, 2009). In piezoresistive readout, a strain sensor is integrated into the cantilever and the applied surface stresses are measured directly, with the mechanical energy transduced into a readily measurable electrical signal. Therefore, piezoresistive method is ideally suited to monitor stresses occurred as cantilever deflected. During the application, the strain sensor will undergo strain expansion or contraction with respect to the applied surface stresses and this

will change the electrical conductivity. The change can be detected and measured with a simple Wheatstone bridge circuit (Johansson et al., 2005). Compared to the capacitive and optical readout method, piezoresistive readout exhibits several advantages like inexpensive, increases the device compatibility, and no external sensor is required. (Brugger et al., 1999). Therefore, the piezoresistive method is selected as readout method in this research.

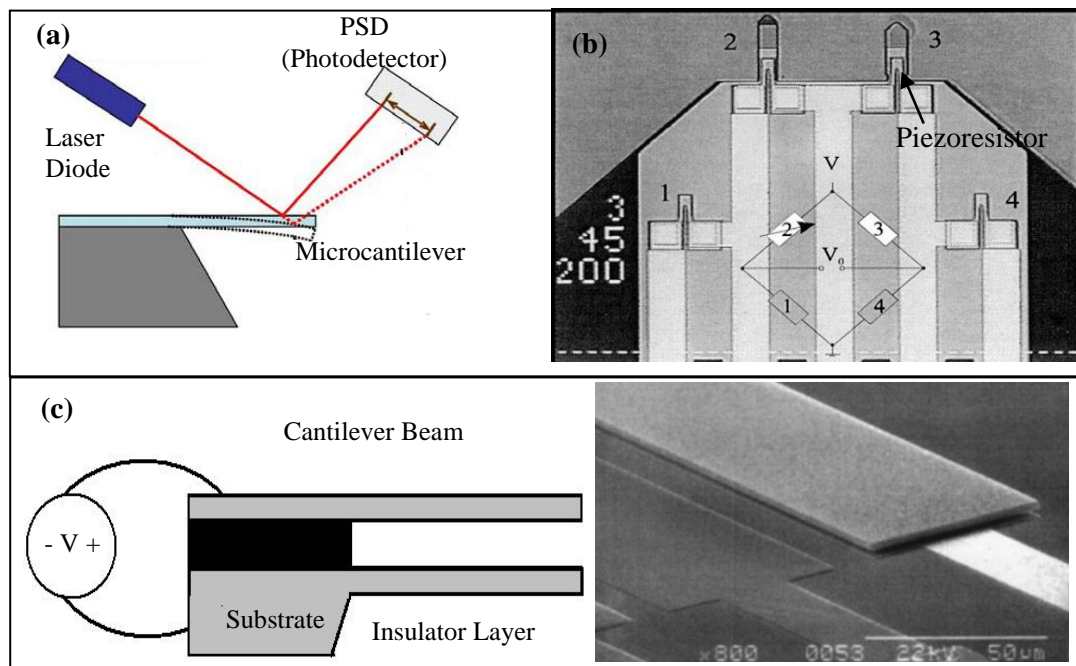


Figure 1.4 Readout Method: (a) optical (Zheng et al., 2008); (b) piezoresistive (Thaysen et al., 2000); (c) capacitive (Napoli et al., 2004)

1.5 Problem Statement

As briefly discussed, the early microcantilever sensors were mostly based on silicon micromachining. However, for biochemical sensing environment, the sensors are always required to be very chemically resistant or biocompatible. Complementing the above requirement, a new technique based on a commercial photoresin namely SU-8 has to be studied and applied.

As microcantilever works through the detection of the deformation, a piezoresistors is integrated with the cantilever to detect any change in the surface stress. Conventionally, silicon has been used as piezoresistive material due to its high gauge factor and thereby high sensitivity to strain changes in a sensor. Unfortunately, Si piezoresistor is hard to be

incorporated in SU-8 microcantilever due to the large Young's modulus of Si (180 GPa) will increase the stiffness of cantilever. In order to maintain the low stiffness of cantilever, the stiffness of the piezoresistor should be low enough compared to the stiffness of SU-8 cantilever. This can only be achieved by reducing the thickness of Si piezoresistor which significantly increases the noise. Therefore, the major challenge for piezoresistive SU-8 microcantilever is to incorporate the piezoresistive material which has gauge factor as high as Si and Young's modulus as low as SU-8, to increase the sensitivity.

Silicon and SU-8 based cantilever are well known consisting of different material configurations. In silicon based piezoresistive microcantilevers, the cantilevers are typically rectangular-shaped bars of Si/ Si₃N₄/ SiO₂ with p-doped or n-doped silicon piezoresistors, while the SU-8 based microcantilevers are usually comprised of SU-8 bars embedded with metallic piezoresistor. Due to the distinct constituent materials, these cantilevers may require different aspects of design optimization. However, compared to silicon based piezoresistive cantilever which was well studied and analyzed by finite element method (Goericke and King, 2008; Chivukula et al., 2006), no published literature that provides a thorough Finite Element Analysis (FEA) for SU-8 cantilevers under surface stress loading which exists during biochemical sensing. Therefore, it is indispensable to implement a series of geometrical analysis for SU-8 cantilevers under surface stress loading, to investigate the relative influence of all the relevant geometrical parameters, including cantilever width, length to width ratio, and piezoresistor placement before proceeding to the fabrication step.

In order to use SU-8 as an alternative structural material to silicon, the sensitivity of fabricated SU-8 piezoresistive microcantilevers need to be comparable to Si based microcantilevers. The design and fabrication techniques of Si cantilever have been well studied and thus it is very difficult to be overtaken. However, there is still huge room of improvement for SU-8 cantilever as it is just getting attention in recent years. Therefore, one of the challenges in this current work is to fabricate the SU-8 piezoresistive microcantilever with sensitivity that can compete to the Si cantilever under surface stress loading.

1.6 Research Objectives

For this project of “SU-8 Piezoresistive Microcantilever for Chemical Sensing Application”, there are three objectives to be achieved:

- To establish a set of design guidelines for maximized surface stress sensitivity of SU-8 piezoresistive cantilevers by using the Finite Element Analysis.
- To fabricate the SU-8 piezoresistive microcantilever with integrated conductive polymer composite for electrical detection.
- To characterize and test the fabricated SU-8 piezoresistive microcantilever under the applied surface stress.

1.7 Thesis Outline

This thesis is presented in six chapters which include introduction, literature reviews, theory, methodology, results and discussion and finally conclusion. The first chapter gives a brief introduction on the microcantilever sensor with an overview of surface stress based biochemical sensor, SU-8 material, and detection method of microcantilever. The problem statements and research objectives are also discussed. The second chapter encompasses gathered literature survey regarding sensor classification, piezoresistive microcantilevers for chemical sensing, and design consideration for piezoresistive microcantilever. This chapter also deals with the past and current trends in the fabrication and numerical analysis of piezoresistive microcantilever. In third chapter the theoretical consideration and analytical model for mechanical bending of cantilever is presented. Using all the gathered information in second and third chapters, chapter four documents the methodology that has been carried out for simulation, fabrication, design and characterization of SU-8 piezoresistive microcantilever. Chapter five presents and discusses the results collected from FEA, fabrication and experiments. Conclusions for this research project have been documented in chapter six. This dissertation ends with recommendation on several future works for designing and fabricating the SU-8 piezoresistive microcantilever.

CHAPTER 2 LITERATURE REVIEW

2.0 Overview

This chapter presents the literature review on the background and prior works related to various components of this work. This review also serves to justify some of the design concept in this study and to understand the issues related to piezoresistive microcantilever-based chemical sensing. The scopes covered are shown as below:

- Sensor classification
- Piezoresistive microcantilevers for chemical sensing
- Design consideration
- Finite element analysis
- Fabrication of SU-8 microcantilevers

2.1 Sensor Classification

Nowadays vast arrays of sensors have been investigated for response to a wide variety of measurands. In order to facilitate obtaining a comprehensive overview of them, a scheme for categorizing sensors is presented. According to White (1987), sensor classification is divided into three categories: physical, chemical, and biological. The following definitions from Hulanicki et al. (1991) will help to clarify the nature and purview of this research:

Physical sensor: A device that provides information about a physical property of the system.

Chemical sensor: A device that transforms chemical information into an analytically useful signal. The chemical information might originate from a chemical reaction of the analyte or from a physical property of the system investigated.

Biological sensor: A biological sensor is a device that is able to transform information on biomass into a useful analytical signal.

Figure 2.1 illustrates the chemical sensing process. The receptor of a chemical sensor transforms the chemical information as an input signal which can be measured by the transducer. The transducer then converts the chemical signal into an analytically useful signal. The receptor of chemical sensors may be based upon various principles, according to Hulanicki et al. (1991):

Physical: The detection is based on the physical change such as absorbance, refractive index, conductivity, mass change, temperature, etc.

Chemical: A chemical reaction occurs with the participation of the analyte resulting in an analytical signal.

Biochemical: A biochemical reaction is the source of analytical signal. These may be considered a subset of chemical receptors, also referred as *biosensor*.

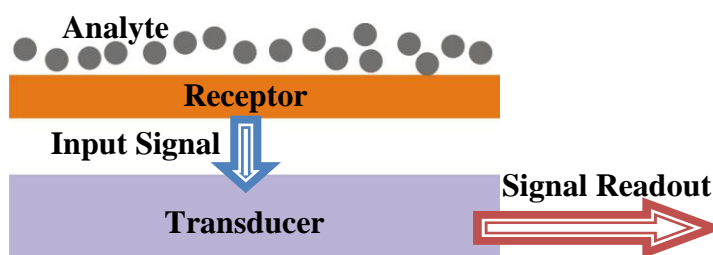


Figure 2.1 Schematic of chemical sensing process

In this work, the chemical sensor with receptor based on the chemical principle is chosen and the gas-phase chemical sensing experiment will be performed. In addition, since the surface stress is induced by chemical and biochemical reaction, this is also categorized as surface stress-based sensor (Satyanarayana, 2005). Surface stress measurement is a label-free method of chemical and biochemical detection and is the main concern in this study as it is chosen as the method of analyte detection.

2.2 Piezoresistive Microcantilever for Chemical Sensing

Microcantilever is an extremely simple yet versatile class of sensors and can also be an excellent platform for chemical and biochemical detection (Lavrik et al., 2004). Since the demonstration of the high sensitivity of microcantilevers by Tortonese et al. (1991) and Thundat et al. (1994), it has been applied to the detection of various analytes. Microcantilever can be operated either in dynamic or static mode. This research utilizes the static mode by measuring the cantilever deflection resulting from surface stress that is generated due to the interaction of analyte with a ‘functionalized’ cantilever surface. Functionalization refers to the surface modification on the top of cantilever so as to allow for selective binding to specific analyte (Choudhury, 2007). As mentioned in **section 1.4**, the cantilever bending due to surface stress on the cantilever can be measured by various detection methods. Most of them infer the surface stress through measuring the cantilever tip deflection using simple beam theory (Gere and Timoshenko, 1997). Piezoresistive is different at that point of view, as the surface stress can be measured directly using a piezoresistive strain gage. The surface stress sensitivity (S) for a cantilever integrated with piezoresistor (resistance, R) under the applied surface stress (σ_s) can be related to the change in resistance ($\Delta R/R$) by:

$$S = \frac{\Delta R}{R} \sigma_s^{-1} \quad (2.2-1)$$

The schematic in **Figure 2.2** demonstrates the selectively binding on functionalized cantilever and the surface stress occurred that results in the change in resistance.

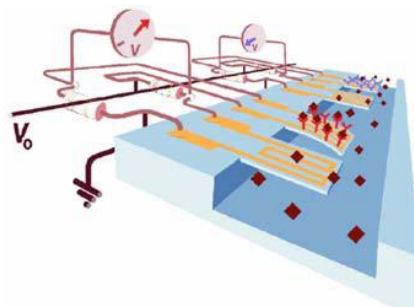


Figure 2.2 Scheme of analyte binds selectively to the functionalized cantilever (Nordström, 2008)

2.2.1 Piezoresistive Readout Concept

In piezoresistive readout (Yang et al., 2003; Meyer et al., 1988), a piezoresistor is embedded onto the cantilever to monitor the stress change on the cantilever. The electrical conductivity of a piezoresistive material changes when stress is applied to it. As the microcantilever deflects, it undergoes a stress change which then result in the change in resistance that can be transduced to the electronic signal. Therefore, the cantilever deflection is proportional to the resistance change if a piezoresistive element is integrated onto the cantilever during fabrication. The integrated readout scheme using piezoresistors has the advantages as the readout system is being compact which facilitates the use in large arrays and the readout scheme is not affected by the optical properties of the liquids in the system (Rasmussen, 2003).

However, for higher electrical characteristic, the thin piezoresistive layer needs to be encapsulated into insulation layer and hence forming multilayer cantilever (Linnemann et al., 1995). The complexity in fabricating the piezoresistive microcantilever is increased due to that embedded piezoresistor, but the on-chip microcantilever sensor integrated with sensor circuit and mechanical system becomes possible (Thaysen et al., 2001). The piezoresistor material in the beam must be located at stress concentration area and as close to the cantilever surface as possible for maximum sensitivity. The resistance of a piezoresistive material changes when strain is applied to it. The relative change in resistance as a function of applied strain can be written as:

$$\frac{\Delta R}{R} = G_{fl}\varepsilon_l + G_{ft}\varepsilon_t \quad (2.2-2)$$

where G_f denotes gauge factor of the material, ε is piezoresistive strain, and the subscripts l and t are terms for longitudinal and transversal respectively. The gauge factor is the intrinsic characteristic of material which can be calculated directly by straining the cantilevers and measuring the resistance change (Vashist, 2007).

2.2.2 Wheatstone Bridge Configuration

In order to measure an electrical signal the piezoresistor on the cantilever is placed in a Wheatstone bridge. **Figure 2.3** illustrates how the circuit converts the change in resistance into a voltage. The output signal V_{out} due to the change in resistance of the variable resistor (cantilever resistor, R_{cant}) in the figure can be determined by using the common Voltage divider formula and is shown as below:

$$V_{out} = \left(\frac{R_2}{R_{cant} + R_2} - \frac{R_3}{R_1 + R_3} \right) V_{in} \quad (2.2-3)$$

The drawbacks to the piezoresistive readout are the signal may suffer from inevitable mechanical or electronic noise and thermal drift due to the current flowing through the cantilever during the operation (Shekhawat et al., 2006). However, Thaysen et al. (2000) has introduced a highly symmetrical Wheatstone bridge configuration to minimize the noise and drift of the output signal.

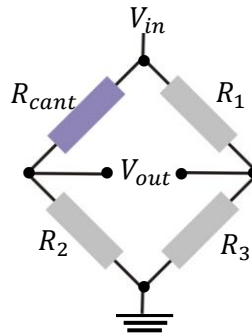


Figure 2.3 Schematic of a Wheatstone bridge. The resistor placed inside the cantilever used for measuring is denoted R_{cant} . The supply voltage is denoted V_{in} and the output voltage V_{out}

Measurements have been carried out for a nonsymmetrical bridge (**Figure 2.3**: one cantilever resistor, three substrate resistors) and a symmetrical bridge (**Figure 2.4**: two cantilever resistors, two substrate resistors). Compared to the nonsymmetrical bridge that exhibits a highly non-linear behavior, the symmetrical bridge configuration is able to reduce drift by two orders of magnitude.

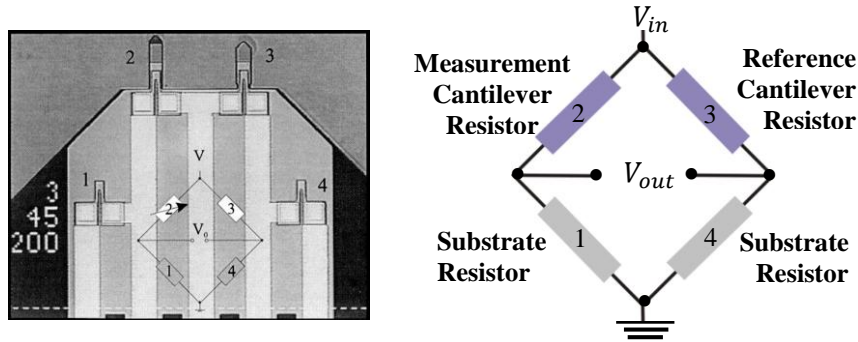


Figure 2.4 Optical microscope image of the thermally symmetrical Wheatstone bridge configuration (Thaysen et al.,2000)

In the symmetrical bridge configuration, one of the cantilevers acts as 'active' cantilever that is used to measure the signal of interest, whereas the reference cantilever filters out the identical signals in both piezoresistors. This design is therefore well suit in cantilever based chemical sensing as the active cantilever reacting with the analyte while the reference cantilever ensures a low drift in the sensing.

2.2.3 Piezoresistive Material

Generally, piezoresistive elements fabricated into cantilevers comprise either semiconductor or metallic strain gauges. The higher gauge factor of semiconductor piezoresistors, such as polysilicon, is definitely an advantage but they are more sensitive to temperature variations in comparison to metallic resistors. Compensation methods must therefore be adopted when using semiconductor strain gauges. Obermeier et al. (1992) and French et al. (1989) have tested the gauge factors (G_f) for boron doped polysilicon (p-type) and the results give $G_f = 20\sim 30$, depending on the doping concentration. These values are about 10 times higher than metallic resistors, which the gauge factor is usually below 2 (Beeby et al., 2004).

The gauge factor of a material with resistivity ρ and Poisson's ratio ν can be expressed by:

$$G_f = \frac{d\rho/\rho}{\varepsilon} + (1 + 2\nu) \quad (2.2-4)$$

where ε is known as strain. This equation indicates clearly that there are two distinct effects that contribute to the gauge factor. The first term is the piezoresistive effect $((d\rho/\rho)/\varepsilon)$ and the second is the geometric effect $(1 + 2\nu)$. For a metallic strain gauge the geometric effect dominates the piezoresistive effect; whereas for a semiconductor the converse is true. As Poisson's ratio is usually between 0.2 and 0.3, the contribution to the gauge factor from the geometric effect is therefore between 1.4 and 1.6, which explained the low gauge factor of metallic strain gauge.

If the geometric effect in silicon piezoresistor is neglected, then the fractional change in resistance is given by **equation 2.2-5** and it can be further simplified by **equation 2.2-6** for p-type silicon, as $\pi_t = -\pi_l$ for p-type silicon.

$$\frac{\Delta R}{R} = \pi_l \sigma_l + \pi_t \sigma_t \quad (2.2-5)$$

$$\frac{\Delta R}{R} = \pi_l (\sigma_l - \sigma_t) \quad (2.2-6)$$

where π_l and π_t are the longitudinal and transverse piezoresistive coefficients and σ_l and σ_t are the corresponding stresses. **Equation 2.2-6** also indicates the resistance change for p-type silicon depends solely on the difference of the induced stress in the lengthwise and widthwise direction.

Doped silicon piezoresistor with high gauge factor is an ideal choice for conventional silicon-based microcantilever. However, the use of silicon piezoresistor may affect the stiffness of polymeric cantilever, i.e. SU-8, due to its large Young's modulus (180 GPa). In case a silicon piezoresistor is integrated into SU-8 cantilever with much lower Young's modulus, the silicon resistor must be thin enough to retain the overall cantilever stiffness, which increases the noise significantly and thereby reducing the signal to noise

ratio (Thayson et al., 2002). Therefore, an alternative piezoresistive material needs to be substituted for polymeric cantilever. SU-8 microcantilevers with an integrated gold strain gauge have been reported earlier (Thayson et al., 2002; Johansson et al., 2005), but are less sensitive due to the fact that gold has a lower gauge factor of around 2.

In recent study (Gammelgaard et al., 2006; Seena et al., 2009), the conducting SU-8 in the form of a SU-8/ Carbon black composite has been used as strain gauge in SU-8 microcantilever, and shows the potential to yield the gauge factor as high as 20. The principle is that when the nano size carbon black reach a certain concentration in the SU-8 (percolation threshold), it forms a conducting network as shown in **Figure 2.5a**. Upon deformation the cantilever is expanded, increasing the distance between the carbon particles and eventually breaking the contact between them (**Figure 2.5b**), resulting in an increase in resistivity of the composite film (Nordström, 2008).

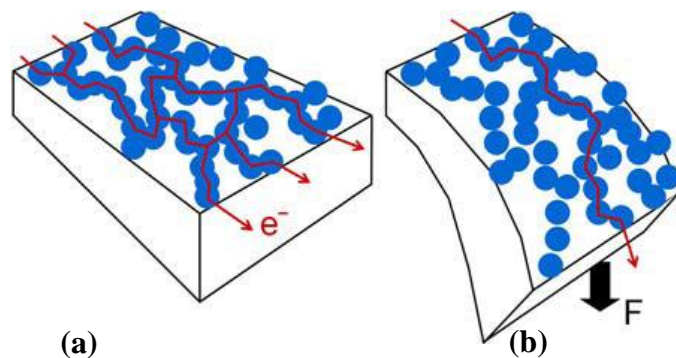


Figure 2.5 As the cantilever is strained, contact is broken between the conducting particles in the polymer and thus increases the resistance (Nordström, 2008)

In view of such a composite strain gauge in combination with the soft SU-8 material has great prospects for highly sensitive polymeric microcantilever sensor, one of the scopes of this work is to integrate the SU-8/ Silver(Ag) composite into SU-8 microcantilever to yield the same or higher gauge factor than SU-8/ Carbon composite. Ag is chosen as it has higher conductivity compared to carbon and SU-8/ Ag with lower percolation threshold (Jiguet et al., 2004) is definitely an economically interesting material especially for volume production.

2.2.4 Existing Piezoresistive Microcantilever for Surface Stress Measurement

Most cantilever sensors used for chemical sensing are based on optical detection of deflection. Due to the limitations of optical readout in numerous liquid phase, the research have been evolved to surface stress detection based on piezoresistive microcantilever detection schemes (McFarland and Colton, 2005; Seena et al., 2009). **Table 2.1** summarizes the existing piezoresistive microcantilever with known surface stress sensitivity, and their corresponding device details and aspects of novelty. Note that the novelty of SU-8 piezoresistive cantilever is often not in the design aspect, as the cantilever design and even fabrication techniques are almost the same. It is clear that the silicon based microcantilevers have a leading sensitivity over polymeric cantilever for past few years until the emerging of SU-8/ Carbon black conductive polymer as the piezoresistors. The sensitivity reported from literatures will be compared with the microcantilever sensor presented in current research work, which will be discussed in detail in **Chapter 5**. Such comparison is important to define the level of achievement of the fabricated sensor.

Table 2.1 Existing piezoresistive microcantilever sensors for surface stress detection

Authors	Device Details	Novel Aspects	Sensitivity (N/m) ⁻¹
Thaysen et al. (2000)	Si based multipurpose microprobes with integrated piezoresistive read-out	- SOI wafers with buried boron etch-stop layers - Highly symmetry Wheatstone bridge	1x10 ⁻³
Thaysen et al. (2002)	SU-8-based cantilever with a gold strain gauge.	- Use of lower Young's modulus of SU-8 for higher surface stress sensitivity	3x10 ⁻⁴
Li et al. (2006)	SOI-based multilayered piezoresistive microcantilever.	- Use of XeF2 for bulk etching of silicon. - SiO ₂ cantilever	8.37x10 ⁻⁴
Choudhury (2007)	Si based cantilever with n-doped piezoresistor.	- n-doped piezoresistor	7.05 x 10 ⁻⁴
Seena et al. (2009)	SU-8 based cantilever with SU-8/CB strain gauge.	- Lower percolation threshold - Less cantilever thickness	4.1x10 ⁻³

2.3 Design Consideration

Design of the piezoresistive microcantilever for surface stress sensing application needs to take the cantilever shape and sensitivity enhancement into account. A significant error in most works on piezoresistive microcantilevers for surface stress sensing is because the cantilevers are designed based on the criterion on AFM application where the designed cantilevers were targeted for both AFM applications and biochemical sensing applications (Antonik et al., 1997; Butt, 1996; Na et al., 2005; Raiteri et al. 1999; Wu et al., 2001). However, these two different applications have fundamentally different mechanical loading conditions. In AFM applications, a tip loading is applied to the cantilever, while in the biochemical sensing applications a surface stress is applied to one surface of the cantilever uniformly. Thus, Goericke and King (2008) have pointed out that cantilevers optimized for AFM application may not be optimal for the other.

Besides, Thaysen (2001) also indicates the surface stress is considered local, which means the stress will not be picked up if the resistors are placed at non-surface stress area. This phenomenon is visualized in **Figure 2.6**, where the cantilever exhibits constant curvature at surface stress area and remains straight at non-surface stress area. Hence it is essential to place the piezoresistor in the region of surface stress when designing the surface stress-based piezoresistive microcantilevers.

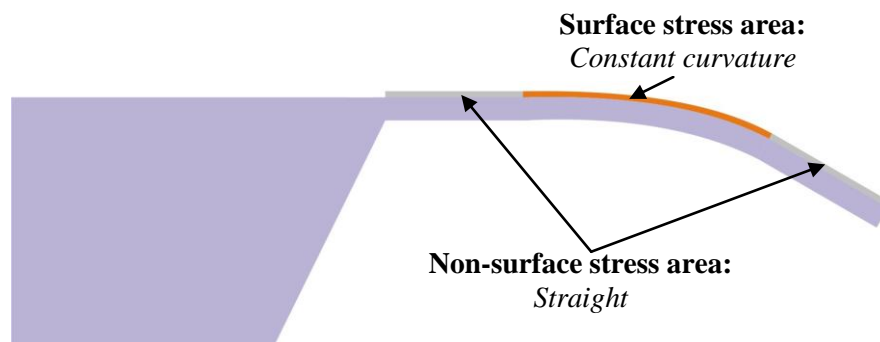


Figure 2.6 The cantilever exhibits a constant curvature in places where surface stress is applied and remains straight at non-surface stress area (Thaysen, 2001)

2.3.1 Cantilever Shape

The cantilever shape often depends upon the readout method and application. **Table 2.2** presents the summary of cantilever shape with their corresponding readout method and application. It can be seen that the U-shaped and V-shaped piezoresistive cantilevers (**Figure 2.7**) are often used in AFM application. In such design the piezoresistor uses the complete surface of cantilever and the cantilever dimensions are being minimized, which thus optimize the force sensitivity and resolution (Tortonese et al., 1991). U-shaped cantilever allows the minimization of the cantilever dimensions, especially its width. If the length to width ratio (L/W) is large enough, the U-shaped cantilever will then behave as two identical separated rectangular cantilevers corresponding to the two legs (Villanueva et al., 2004).

The rectangular and paddle type (**Figure 2.7**) cantilevers are commonly used in optical detection method. However, the beam curvature by surface stress is not uniform as the cantilever beam is clamped at one end, and this causes the beam to twist, which then induces large cantilever initial curvatures and high divergence of the reflected laser beam, significantly decreasing the sensitivity. Therefore, Plaza et al. (2006) proposed the T-shaped (**Figure 2.7**) microcantilever array to reduced initial angular offset and angle deviation between the cantilevers array. This design allows the beam to be mechanically decoupled from the twist-inducing stress at the clamped end.

Besides, the paddle type piezoresistive cantilevers are also commonly used in flow sensing application, as the typical flow sensor consists of three elements; a channel, cantilevers with a rectangular plate paddle and piezoresistive material implanted into the cantilevers (Mahalik, 2008). For the rectangular type, it is undeniably the universal to surface stress-based cantilever sensor, especially in piezoresistive detection method. Compared to rectangular cantilever, the U-shaped, V-shaped and paddle type cantilever are designed to optimize the sensitivity for AFM application. The common ground of these designs is the piezoresistors are placed along the long and skinny arms, which are not necessarily appropriate for stress-sensing cantilever sensors, especially for p-doped silicon (Goericke and King, 2008).

Table 2.2 Summary of cantilever shape from literatures

Authors	Cantilever Shape	Readout Method	Applications
A lvarez and Tamayo (2005)	Rectangular	Optical	Biosensor
Baselt et al. (2003)	Rectangular	Capacitive	Hydrogen sensor
Bashir et al. (2000)	U-shaped	Piezoresistive	AFM
Behrens et al. (2003)	U-shaped & Rectangular	Piezoresistive	AFM
Chivukula et al. (2006)	Rectangular	Piezoresistive	Surface stress sensing
Choudhury et al. (2007)	Rectangular	Piezoresistive	Surface stress sensing
Fan et al. (2002)	Paddle type	Piezoresistive	Flow sensor
Fletcher et al. (2008)	T-shaped	Piezoresistive	Gas sensor
Johansson et al. (2005)	Rectangular	Piezoresistive	Surface stress sensing
Kim et al. (2000)	Paddle type	Piezoresistive	Flow sensor
Lang et al. (1998)	Rectangular	Optical	Chemical sensor
Linnemann et al. (1995)	Rectangular	Piezoresistive	AFM
Loui et al. (2008)	Rectangular, Square, trapezoidal	Piezoresistive	Surface stress sensing
Na et al. (2005)	Rectangular	Piezoresistive	Biosensor
Plaza et al. (2006)	T-shaped	Optical	Biosensor
Ransley et al. (2006)	Rectangular	Optical	Bio-chemical sensor
Rasmussen et al. (2003)	Rectangular	Piezoresistive	Biosensor
Saya et al. (2005)	V-shaped	Piezoresistive	AFM
Seena et al. (2009)	Rectangular	Piezoresistive	Surface stress sensing
Sone et al. (2004)	V-shaped	Piezoresistive	Biosensor
Su et al. (1996)	Paddle type	Piezoresistive	Flow sensor
Thaysen et al. (2000)	Rectangular	Piezoresistive	AFM
Thaysen et al. (2001)	Rectangular	Piezoresistive	Bio-chemical sensor
Thaysen et al. (2002)	Rectangular	Piezoresistive	Surface stress sensing
Tortonese et al. (1991)	U-shaped	Piezoresistive	AFM
Verd et al. (2005)	Rectangular	Capacitive	Resonator
Villanueva et al. (2004)	U-shaped	Piezoresistive	Force sensor
Yang et al. (2010)	Rectangular	Piezoresistive	Chemical sensor
Yu et al. (2001)	Rectangular	Piezoresistive	Surface stress sensing
Yue et al. (2004)	Paddle type	Optical	Biosensor
Zhang & Xu (2004)	Rectangular	Optical	Biosensor
Zhou et al. (2009)	Rectangular	Piezoresistive	Surface stress sensing

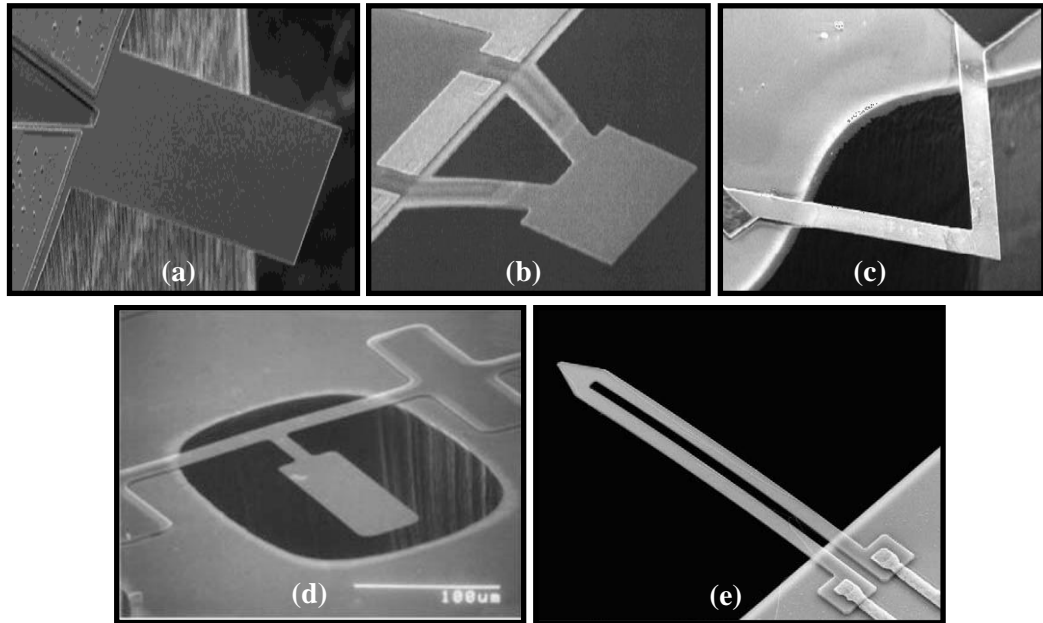


Figure 2.7 Types of microcantilever shape, (a) Rectangular (Loui et al., 2008), (b) Paddle type (Su et al., 1996), (c) V-shaped (Saya et al., 2005), (d) T-shaped (Plaza et al., 2006), (e) U-shaped (Villanueva et al., 2004)

Therefore, from the literature that is summarized in **Table 2.2**, the conventional rectangular cantilever is chosen for this research work, due to its simplicity in fabrication and suitability in surface stress sensing application.

2.3.2 Sensitivity Enhancement

There are several ways to enhance the sensitivity of piezoresistive microcantilever as proposed in published literature. **Table 2.3** summarizes the available approaches for the purpose mentioned. The ways for sensitivity enhancement can be categorized as: (i) Geometrical Optimization; (ii) Stress Concentration Region; (iii) Material Changing; and (iv) Special Design.

i. Geometrical Optimization

Conventional wisdom by changing the geometrical parameters is imperative and the simplest way to increase the cantilever sensitivity under applied surface stress. The changeable parameters include the cantilever length, width, and thickness, and piezoresistor size, location, and thickness. For example, Goericke and King (2008) have concluded the

cantilever length is not critical for high sensitivity while the piezoresistor length should be minimized to reduce overall resistance and increase device sensitivity, for the case of p-type silicon. Chivukula et al. (2006) have also demonstrated the highest sensitivity can be obtained when the piezoresistor length is approximately 2/5 of the silicon dioxide (SiO₂) cantilever length. Furthermore, Thaysen (2001) has performed a complete derivation of the surface stress sensitivity for multilayer cantilever, which can be utilized to optimize the thickness for each cantilever layer.

ii. Stress Concentration Region (SCR)

SCR is the result of discontinuities such as holes, grooves, keyways, cracks or sharp change in one of the dimensions of the structure (He and Li, 2006). These structural discontinuities enhance the stress around their proximity. A few groups have devoted their time to the enhancement of the surface stress via SCR. Yu et al. (2007) designed six rectangular holes on the piezoresistive region of the cantilever, and the measurement results showed a 1.3 times increase in cantilever displacement sensitivity. Bhatti et al., (2007) modeled the effect of different number and position of holes added to the piezoresistive paddle cantilever sensors using the finite element analysis. However, most of the literatures regarding to SCR optimize the displacement sensitivity, in which for surface stress-based piezoresistive cantilever the deflection is not monitored and thus not the best indicator of sensitivity.

As described in **Section 2.2.3**, the surface stress sensitivity depends solely on the difference of the induced piezoresistive stress ($\sigma_l - \sigma_t$), but the stress σ_l and σ_t are amplified simultaneously by the biaxial surface stress loading and therefore such SCR design is by no means beneficial to surface stress sensitivity.(Yang and Yin, 2007). Furthermore, the design of SCR increases the complexity of fabrication steps such as alignment accuracy during the lithography and this explained why most of previous literatures remain on the analysis stage.

iii. Material Changing

As shown in **equation 2.2**, the cantilever sensitivity is proportional to the strain ϵ induced by the surface stress or inversely proportional to the Young's modulus E of the cantilever material. Nowadays major microcantilever sensors for biochemical sensing application were made in silicon. Due to the relative large Young's modulus of silicon material, the bending response of the silicon microcantilever is too weak to be measured when the surface stress change is rather small. Therefore, by changing the structural material with much lower Young's modulus, a higher mechanical sensitivity would be expected. For example, Tang et al. (2003) reported that SiO_2 microcantilevers offer approximately 20-fold bending response compared to the same dimensions silicon microcantilevers with the same surface stress applied. The SU-8 polymer, which is a high aspect ratio negative photoresist, has arisen as a promising substitute to the silicon as the cantilever structural material (Thaysen et al., 2002). The SU-8 cantilever even shows greater surface stress sensitivity over the silicon based cantilever in recent study (Seena et al., 2009).

iv. Special Design

The special design is often used to suit the cantilever for biaxial surface stress sensing application. The design is in no term of cantilever shape or geometrical parameter of conventional rectangular cantilever, but the change of entire cantilever structures. An interesting example would be the double microcantilever (**Figure 2.8**) invented by Yang et al. in 2006. The double-microcantilever is composed of a top functionalized cantilever and another bottom measuring cantilever such that the biaxial surface stress in the former can be converted into uniaxial strain in the latter. In addition, the temperature increase during sensor operation is isolated from the functionalized cantilever and thereby the biochemical agent (i.e. protein) will not be affected. However, the sensitivity of the cantilever highly depends upon the transmitter rigidity and the fabrication process inevitably becomes extremely difficult which results in the low reproducibility.

Table 2.3 Summary of available approaches in enhance the sensitivity

Approach	Authors
Geometrical Optimization	Goericke and King (2008); Chivukula et al., (2006); Thaysen (2001); Loui et al. (2008)
SCR	Bashir et al. (2000); He and Li, (2006); Yu et al. (2007); . Bhatti et al., (2007); Ansari and Cho (2008)
Material Changing	Tang et al. (2003); Thaysen et al.,(2002); Seena et al., (2009); Johansson et al. (2005); Gammelgaard et al. (2006); Seena et al. (2009); Chen et al. (2008)
Special Design	Yang and Yin, (2007); Yang et al. (2006)

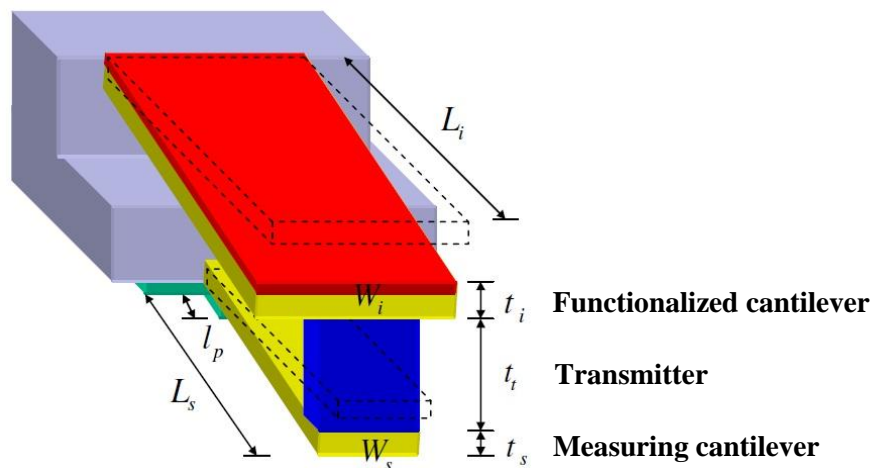


Figure 2.8 The double-microcantilever design composed of the functionalized microcantilever, measuring microcantilever, and the connecting transmitter (Yang et al., 2006)

2.4 Finite Element Analysis

In many researches, computer aided design (CAD) and finite element software have been employed to analyze MEMS structures prior fabricating the microdevice. By running FEA, a preliminary understanding on the cantilever performance such as stress distribution and deflection will be made possible. Furthermore, FEA will help in reducing design revisions and the time consumed during the design stage. Currently, there are two most popular analysis tools for microcantilever sensor, which are CoventorWareTM and ANSYS®.

CoventorWareTM software has functionality that allows the integrating of modeling and fabrication process. Several researchers have proved the ability of CoventorwareTM in analyzing the sensor designed. For instance, Chivukula et al, (2006) has utilized CoventorWareTM for optimization of SiO₂-based piezoresistive microcantilever by varying piezoresistor geometries and doping concentration, while Don and Tuantranont (2005) used CoventorWareTM to study the effect of biochemical adsorption on cantilever surface.

However, most of the researchers utilize ANSYS® software for devices analyzing, due to the fact that CoventorWareTM is expensive and has some limitations in the analysis study. For piezoresistive microcantilever, many researchers used ANSYS® to study the device behavior such as piezoresistive strain and resistance change for design optimization. Yu et al. (2005) has employed ANSYS® in analysing the stress distribution and vertical displacement for the Si piezoresistive cantilever with stress concentration holes. Yang and Yin (2007) has studied the effect of thermal stress to the piezoresistive strain induced in Si cantilever.

Table 2.4 summarized literatures that used ANSYS® for piezoresistive microcantilever analysis under surface stress loading. Note that most of the researchers used the equivalent moment loading on the cantilever free edge calculated using Sader equation (Sader, 2001) to model the surface stress loading. However, such equivalent boundary condition totally ignores the effect of transverse stress, which occurred in biaxial surface stress. In view of this, Goericke and King (2008) has loaded the cantilever top surface with